physics

MDPI

Article

Entropy Production Due to Electroweak Phase Transition in the Framework of Two Higgs Doublet Model

Arnab Chaudhuri [1,*] and Maxim Yu. Khlopov [2,3,4]

1 Department of Physics and Astronomy, Novosibirsk State University, Lyapunova 2, 630090 Novosibirsk, Russia
2 Institute of Physics, Southern Federal University, 344090 Rostov on Don, Russia; khlopov@apc.in2p3.fr
3 CNRS, Astroparticule et Cosmologie, Université de Paris, F-75013 Paris, France
4 Center for Cosmopartilce Physics "Cosmion", National Research Nuclear University "MEPhI" (Moscow Engineering Physics Institute), 115409 Moscow, Russia
* Correspondence: arnabchaudhuri.7@gmail.com

Abstract: We revisit the possibility of first order electroweak phase transition (EWPT) in one of the simplest extensions of the Standard Model scalar sector, namely the two-Higgs-doublet model (2HDM). We take into account the ensuing constraints from the electroweak precision tests, Higgs signal strengths and the recent LHC bounds from direct scalar searches. By studying the vacuum transition in 2HDM, we discuss in detail the entropy released in the first order EWPT in various parameter planes of a 2HDM.

Keywords: electroweak phase transition; 2HDM; extended Standard Model; entropy

check for updates

Citation: Chaudhuri, A.; Khlopov, M.Y. Entropy Production Due to Electroweak Phase Transition in the Framework of Two Higgs Doublet Model. *Physics* **2021**, *3*, 275–289. https://doi.org/10.3390/physics3020020

Received: 4 March 2021
Accepted: 19 April 2021
Published: 29 April 2021

Publisher's Note: MDPI stays neutral with regard to jurisdictional claims in published maps and institutional affiliations.

Copyright: © 2021 by the authors. Licensee MDPI, Basel, Switzerland. This article is an open access article distributed under the terms and conditions of the Creative Commons Attribution (CC BY) license (https://creativecommons.org/licenses/by/4.0/).

1. Introduction

It is a well-established fact that electroweak phase transition (EWPT) is either a second order or a smooth crossover in the Standard Model (SM) of particle physics. It is also well-established that the entropy density in the early universe plasma is conserved in the course of the cosmological expansion if the plasma is in thermal equilibrium state with negligible chemical potential of every species [1,2]. The entropy conservation law is given by

$$s = \frac{P+\rho}{T} a^3 = \text{const.} \tag{1}$$

where s is the entropy density, $a(t)$ is the scale factor, $T(t)$ is the temperature of the fluid (or plasma) are function of time t, ρ and P are the energy density and pressure of the plasma, respectively.

In the early universe, the state of matter is quite close to the equilibrium as the reaction rate $\Gamma \sim n\sigma v$, $n = 1, 2$, represents decays of one and two-body reactions, respectively, σv is the product of annihilation cross section, is much faster than the cosmological expansion rate, i.e., the Hubble parameter $\mathcal{H} = \dot{a}/a \propto T^2/m_{Pl}$, where $\dot{a}$ is the time derivative of the scale factor. The equilibrium condition $\Gamma > \mathcal{H}$ is always satisfied for at temperature $T < \alpha\, m_{\rm Pl}$. Here α is the coupling constant of the particle interaction of the order of $\sim 10^{-2}$ and $m_{\rm Pl}$ is the Planck mass. Due to the large value of $m_{\rm Pl}$, thermal equilibrium exists in most of the history of the universe, if $\alpha \ll 1$.

As mentioned above, during thermal equilibrium, the entropy density in the comoving volume is conserved. However, there are scenarios where the entropy density is not conserved. For example, if the universe at a certain stage was dominated by primordial black holes [3], the entropy production can be very high, high enough to delete the pre-existing baryon asymmetry [4]. In the context of the modern cosmological paradigm of inflationary Universe with baryosynthesis and dark matter/energy, physics beyond the

Standard Model (BSM) underlying these necessary elements of the modern cosmological model can provide many examples of various mechanisms of high entropy production (see e.g., [5] for review and references). Taking apart the wide range of various possibilities we consider here the problem of entropy production by minimal extension of SM and start the discussion from the SM predictions for the cosmological entropy production.

A large entropy production could take place during during quantum chromodynamical (QCD) phase phase transition at $T \sim 100$–200 MeV. However, due to difficulty in numerical computation, QCD phase transition in early universe cosmology is not known in detail. For reference, see Ref. [6].

Few mechanisms of realistic though very weak entropy production could take place during the freeze-out of dark matter (DM) particles. However, usually, the fraction of DM density was quite low at the freezing out temperature and the effect is tiny.

An interesting effect, not covered in this paper, is the formation of bubble walls that can take place in the early universe. Their collision can lead to the formation of primordial black holes due to first order phase transition with background gravitational waves [7,8]. The entropy released in the process can wipe out the dark matter density that was present before EWPT. Recent results on muon $(g-2)$ experiment, see Refs. [9–11], have opened up a new window to study dark matter in the framework of extended SM physics which shall be done in our next work.

Most probably, the largest entropy release in the standard model took place in the process of the electroweak transition from symmetric to asymmetric electroweak phase in the course of the cosmological cooling down. In the SM with one Higgs field, the process is a mild crossover and the entropy production is about 13% [12].

According to the electroweak (EW) theory at the temperature higher than a critical one, $T > T_c$, the expectation value of the Higgs field, $\langle\phi\rangle$, in the fluid (plasma) is zero and the universe is in electroweak symmetric phase [13].When the temperature drops below $\langle T_c\rangle$, a nonzero expectation value is created, which gradually rises, with decreasing temperature, up to the vacuum expectation value η. Such a state does not satisfy the conditions necessary for the entropy conservation and an entropy production is expected.

A huge amount of entropy is released if EWPT is first order, which is the case even with the minimalist extension of standard model known as two-Higgs-doublet Model (2HDM). In what follows, we have considered a real 2HDM of type-I and are scanned over certain parameter spaces and used numerical analysis to calculate the entropy production for some interesting and unique benchmark points.

The paper is arranged as follows: in the next section details about 2HDM are given along with some some Large Hadron Collider (LHC) constraints, followed by the theoretical framework of the process. Due to cumbersome and very difficult analytical calculations, we did numerical analysis of certain parameters using the BSMPT package [14]. A generic discussion and conclusion is given there after. The paper closes by two appendices that give details about the metric being used here and also the masses of the scalar bosons generated by 2HDM.

2. 2HDM: A Brief Review and Current Constraints

There are two scalar doublets in the framework and they are defined as:

$$\varphi_I = \begin{pmatrix} \phi_I^+ \\ \frac{1}{\sqrt{2}}(v_I + \rho_I) + i\,\eta_I \end{pmatrix}, \tag{2}$$

with $I = 1, 2$. Here $\phi_I^\pm$, ρ_I, η_I, and v_I indicate the charged, neutral CP-even and neutral CP-odd degrees of freedom (d.o.f.) and the vacuum expectation value (VEV) of the I-th doublet, respectively.

Prior to spontaneous symmetry breaking (SSB), the tree-level 2HDM Lagrangian, comprising of 6-dimensional operators, assumes the form

$$\mathcal{L} = \mathcal{L}_{\text{kin}} + \mathcal{L}_{\text{Yuk}} - V(\varphi_1, \varphi_2) + \mathcal{L}_6, \tag{3}$$

where,

$$\begin{aligned}
\mathcal{L}_{\text{kin}} &= -\frac{1}{4}\sum_{X=G^a,W^i,B} X_{\mu\nu}X^{\mu\nu} + \sum_{I=1,2}|D_\mu\varphi_I|^2 + \sum_{\psi=Q,L,u,d,l}\bar{\psi}i\not{D}\psi, \\
\mathcal{L}_{\text{Yuk}} &= \sum_{I=1,2} Y_I^e\,\bar{l}\,e\varphi_I + \sum_{I=1,2} Y_I^d\,\bar{q}\,d\varphi_I + \sum_{I=1,2} Y_I^u\,\bar{q}\,u\tilde{\varphi}_I, \\
V(\varphi_1,\varphi_2) &= m_{11}^2|\varphi_1|^2 + m_{22}^2|\varphi_2|^2 - (\mu^2\varphi_1^\dagger\varphi_2 + \text{h.c.}) + \lambda_1|\varphi_1|^4 + \lambda_2|\varphi_2|^4 + \lambda_3|\varphi_1|^2|\varphi_2|^2 \\
&\quad + \lambda_4|\varphi_1^\dagger\varphi_2|^2 + \left[\left(\frac{\lambda_5}{2}\varphi_1^\dagger\varphi_2 + \lambda_6|\varphi_1|^2 + \lambda_7|\varphi_2|^2\right)\varphi_1^\dagger\varphi_2 + \text{h.c.}\right], \\
\mathcal{L}_6 &= \sum_i c_i O_i/f^2.
\end{aligned} \tag{4}$$

$\mathcal{L}_{\text{kin}}$ is the kinetic term of the Lagrangian, $\mathcal{L}_{\text{Yuk}}$ is the Lagrangian originating from the Yukawa interaction. The indices $\mu, \nu = 0, 1, 2, 3$ are the indexes for the time-space components. W_i, $i = 1, 2, 3$, and B are the four gauge bosons, G^a $(a = 1, 2)$ are the Goldstone bosons and Y^e, Y^d and Y^u are the Yukawa coupling constants. D is the covariant derivative, see Ref. [15], and q, u, d, e, l, $q, m11, m22$ are defined in Appendix B. The term 'h.c.' and the symbol † stay for the Hermitian conjugate. c_i is the Wilson coefficient of the 6-dimensinal operator O_i and f. The terms proportional to $\lambda_{6,7}$ are known as 'hard-Z_2 violating' because, not only do they lead to a quadratically divergent amplitude for $\varphi_1 \leftrightarrow \varphi_2$ transition [16] but also to CP-violation in the scalar sector for complex values [17]. However, it is possible to realize the CP-conserving limit with nonzero values of $\lambda_{6,7}$ as well [18]. In this paper, we contain our discussion to the CP-conserving 2HDM, and hence $\lambda_{6,7} = 0$. The electroweak symmetry is broken by the VEVs, namely v_1 and v_2 corresponding to the two doublets $\varphi_{1,2}$ respectively. This leads to the mixing of same types of degrees of freedom of $\varphi_{1,2}$. For the case of CP-conservation, the mass matrices of the neutral CP-even and odd scalars and the charged scalars are diagonalized by the following operation:

$$\begin{pmatrix} H \\ h \end{pmatrix} = R(\alpha)\begin{pmatrix} \rho_1 \\ \rho_2 \end{pmatrix}, \quad \begin{pmatrix} W_L^\pm \\ H^\pm \end{pmatrix} = R(\beta)\begin{pmatrix} \phi_1^\pm \\ \phi_2^\pm \end{pmatrix}, \quad \begin{pmatrix} Z_L \\ A \end{pmatrix} = R(\beta)\begin{pmatrix} \eta_1 \\ \eta_2 \end{pmatrix}. \tag{5}$$

Here,

$$R(\theta) = \begin{bmatrix} \cos\theta & \sin\theta \\ -\sin\theta & \cos\theta \end{bmatrix}, \tag{6}$$

h, H are the neutral CP-even physical d.o.f., and A and $H^\pm$ are the neutral CP-odd and charged d.o.f., respectively. Z_L and A are the other scalars. From Equation (5) it can be seen that β is the mixing angle of the charged and CP-odd sectors and is given by $\beta = \tan^{-1}(v_2/v_1)$. Δ is the mixing angle of the CP-even neutral scalars and is expressed as

$$\Delta = \sin^{-1}\left[\frac{\mathcal{M}_{\rho 12}^2}{\sqrt{(\mathcal{M}_{\rho 12}^2)^2 + (\mathcal{M}_{\rho 11}^2 - m_h^2)^2}}\right], \tag{7}$$

with $\mathcal{M}_\rho^2$ is the mass-squared matrix in the neutral CP-even sector and the repeating and non-repeating indices refers to the diagonal and off diagonal elements, respectively. Please see Appendix B for detailed values of the masses. Here, we have assumed that h is the SM-like Higgs with mass of $m_h \sim 125.09$ GeV and $m_H > m_h$. It has been shown that the tree-level Higgs-mediated flavor-changing neutral currents (FCNC) appear in models

where more than one scalar doublet gives mass to the same kind of SM fermions [19,20]. Such a situation can be avoided under the framework of various discrete symmetries, for example, a Z_2 symmetry [19,20].

Due to the rotation in the scalar sector following Equation (5), the couplings of the SM gauge bosons and fermions to the SM-like Higgs boson are required to be re-scaled compared to the corresponding SM values. After SSB, the Yukawa sector of the 2HDM can be written as:

$$\begin{aligned} -\mathcal{L}_{\text{Yuk}} \;=\; & \frac{1}{\sqrt{2}}(\kappa_D s_{\beta-\alpha} + \rho_D c_{\beta-\alpha})\bar{D}Dh + \frac{1}{\sqrt{2}}(\kappa_D c_{\beta-\alpha} - \rho_D s_{\beta-\alpha})\bar{D}DH \\ & + \frac{1}{\sqrt{2}}(\kappa_U s_{\beta-\alpha} + \rho_U c_{\beta-\alpha})\bar{U}Uh + \frac{1}{\sqrt{2}}(\kappa_U c_{\beta-\alpha} - \rho_U s_{\beta-\alpha})\bar{U}UH \\ & + \frac{1}{\sqrt{2}}(\kappa_L s_{\beta-\alpha} - \rho_L c_{\beta-\alpha})\bar{L}Lh + \frac{1}{\sqrt{2}}(\kappa_L c_{\beta-\alpha} - \rho_L s_{\beta-\alpha})\bar{L}LH \\ & - \frac{i}{\sqrt{2}}\bar{U}\gamma_5\rho_U UA + \frac{i}{\sqrt{2}}\bar{D}\gamma_5\rho_D DA + \frac{i}{\sqrt{2}}\bar{L}\gamma_5\rho_L LA \\ & + \Big(\bar{U}(V_{\text{CKM}}\rho_D P_R - \rho_U V_{\text{CKM}} P_L)DH^+ + \bar{\nu}\rho_L P_R L H^+ + \text{h.c.}\Big). \end{aligned} \tag{8}$$

Here, $\kappa_f = \sqrt{2}M_f/v$ for $f = U, D$ and L. L and R are defined after Equation (11). For details of other parameters see Ref. [21]. The generation indices of the fermionic fields have been suppressed in Equation (9). As mentioned earlier, the measurement of the signal strengths of the SM-like Higgs at LHC demands that the properties of one of the neutral CP-even neutral scalars, here h, should closely resemble that of the SM Higgs. As Equation (9) indicates, this is satisfied at the vicinity of the so-called 'alignment limit', i.e., $\cos(\beta - \alpha) \to 0$. The current measurement of Higgs signal strengths have pushed the 2HDMs close to the alignment limit [22–25]. The measurement of the Higgs signal strengths dictate that for type-II 2HDM, at $\tan\beta \sim 1$, the constraint on $\cos(\beta - \alpha)$ is given by $-0.05 \lesssim \cos(\beta - \alpha) \lesssim 0.15$ at 95% CL. The allowed region becomes even smaller for higher values of $\tan\beta$. The situation for type-III and -IV are quite similar to that of type-II 2HDM.

This constraint is comparably relaxed in type-I 2HDM, where the allowed range is $|\cos(\beta - \alpha)| \lesssim 0.4$. Among the tree-level scalar-gauge couplings which are important for the cascade decays of the new scalars, AZh and $H^{\pm}hW^{\mp}$ are proportional to $\cos(\beta - \alpha)$, whereas AZH and $H^{\pm}HW^{\mp}$ are proportional to $\sin(\beta - \alpha)$. The tripple letters denote tripple coupling and Z is one of the SM guage bosons. It is possible to realize an exact alignment in the multi-Higgs-doublet models in the framework of certain additional symmetries of the 2HDM potential [26–30].

The impact of the measurement of the Higgs signal strengths in each individual search channels on the $\cos(\beta - \alpha)$ vs. $\tan\beta$ plane has been discussed in Ref. [31]. It should be mentioned that the coupling multipliers of the SM-like Higgs also becomes close to unity when $\sin(\beta + \alpha) = 1$, i.e., at the so-called 'wrong-sign Yukawa' limit [32] for type-II, type-III, and type-IV 2HDM. Though, with better measurement of the processes like $Vh \to b\bar{b}$, $h \to \gamma\gamma, \Upsilon\gamma$, (where b is the bottom quark), [33,34] the fate of the wrong-sign Yukawa region will be decided in near future.

It is possible to constrain the parameter space of the type-II 2HDM even at the alignment limit from the nonobservation of the heavier scalars [18] in processes like $gg/b\bar{b} \to H/A \to \tau\bar{\tau}, \gamma\gamma, gg \to H \to hh$, etc. Here g and τ represents gluon and tau and their respective interactions. Both ATLAS and CMS experiments are involved in numerous dedicated searches of these kinds, for instance Refs. [35–39], resulting in significant constraints on the 2HDM parameter space.

The constraints from the decay of the new scalars into SM particles are significantly relaxed in the hierarchical scenario compared to the degenerate case [25]. However. for the hierarchical spectrum of new scalars, the channels like $H(A) \to ZA(H)$ dominates the total decay width of such states, leading to new bounds on the parameter space which

are not applicable for the degenerate case. A hierarchical spectrum such as $m_A > m_H \sim m_{H^\pm} \sim v$ can lead to a first order electroweak phase transition providing an explanation for the matter-antimatter asymmetry, with $A \to ZH$ being its smoking gun signature at LHC [40,41]. In general, the importance of Higgs cascade decays as the possible probes of an extended scalar sector have been discussed in the literature [42–47] and $A \to ZH$ decay is dubbed as a 'golden channel' in this context [48].

3. EWPT Theory in 2HDM

The Lagrangian density of the electroweak theory (discussed in details in the previous section) in 2HDM can be expressed as [15]

$$\mathcal{L} = \mathcal{L}_f + \mathcal{L}_{\text{Yuk}} + \mathcal{L}_{\text{gauge,kin}} + \mathcal{L}_{\text{Higgs}}. \tag{9}$$

The first term on the right hand side, $\mathcal{L}_f$, is the kinetic term for the fermion fields:

$$\mathcal{L}_f = \sum_j i\left(\bar{\Psi}_L^{(j)} \not{D} \Psi_L^{(j)} + \bar{\Psi}_R^{(j)} \not{D} \Psi_R^{(j)}\right) \tag{10}$$

$$= i\bar{\Psi}_L \gamma^\mu (\partial_\mu + igW_\mu + ig' Y_L B_\mu)\Psi_L + i\bar{\Psi}_R \gamma^\mu (\partial_\mu + igW_\mu + ig' Y_R B_\mu)\Psi_R, \tag{11}$$

where L and R represents the left and right chiral field of that fermion and $\not{D}$ is the Feynman operator applied on the covariant derivative (it is defined as $\not{A} = \gamma^\mu A_\mu$, where γ are the gamma matrices) [15] and j runs over all fermionic species (the field Ψ_j) listed in Table A1. And g is the coupling constant. The partial derivative denotes derivative over space time, e.g., $\partial_0 = d/dt$ and μ runs from 0 to 3.

The second term of Equation (9), Yukawa interaction term (for details, see previous section), $\mathcal{L}_{\text{Yuk}}$ is [49]

$$\mathcal{L}_{\text{Yuk}} = -\left[y_e \bar{e_R} \Phi_a^\dagger L_L + y_e^* \bar{L_L} \Phi_a^\dagger e_R + \cdots\right], \tag{12}$$

where y_e is a complex dimensionless constant, Φ_a ($a = 1, 2$) is a $SU(2)_L$ doublet and for the Lagrangian to be gauge invariant it is coupled with another $SU(2)_L$ fermion L_L. e_R is the right chiral electron field and the same goes for other fermions like quarks, neutrinos, etc.

The third term $\mathcal{L}_{\text{gauge,kin}}$ represents $U(1)$ invariant kinetic term of four gauge bosons (W^i, $i = 1, 2, 3$ and B). It can be written as

$$\mathcal{L}_{\text{gauge,kin}} = -\frac{1}{4} G^i_{\mu\nu} G^{i\mu\nu} - \frac{1}{4} F^B_{\mu\nu} F^{B\mu\nu}, \tag{13}$$

where $G^i_{\mu\nu} = \partial_\mu W^i_\nu - \partial_\nu W^i_\mu - g\epsilon^{ijk} W^j_\mu W^k_\nu$ and $F^B_{\mu\nu} = \partial_\mu B_\nu - \partial_\nu B_\mu$.

The Lagragian density for the doublet Higgs bosons is given by

$$\begin{aligned} \mathcal{L}_{\text{Higgs}} &= (D^\mu \Phi_1)^\dagger (D_\mu \Phi_2) + (D^\mu \Phi_1)^\dagger (D_\mu \Phi_2) - V_{\text{tot}}(\Phi_1, \Phi_2) \\ &= \{(\partial_\mu + igT^i W^i_\mu + ig' Y B_\mu)\Phi_1\}^\dagger \{(\partial_\mu + igT^i W^i_\mu + ig' Y B_\mu)\Phi_1\} \\ &\quad + \{(\partial_\mu + igT^i W^i_\mu + ig' Y B_\mu)\Phi_2\}^\dagger \{(\partial_\mu + igT^i W^i_\mu + ig' Y B_\mu)\Phi_2\} - V_{\text{tot}}(\Phi_1, \Phi_2, T). \end{aligned} \tag{14}$$

We define

$$\mathcal{W}_\mu = gT^i W^i_\mu + g' Y B_\mu. \tag{15}$$

Thus, from Equation (15), we get:

$$\mathcal{L}_{\text{Higgs,kin}} = (\partial^\mu {\Phi_a}^\dagger)(\partial_\mu \Phi_a) - i(\mathcal{W}^\mu \Phi_a)^\dagger (\partial_\mu \Phi_a) + i(\partial^\mu {\Phi_a}^\dagger)\mathcal{W}_\mu \Phi_a + (\mathcal{W}^\mu \Phi_a)^\dagger \mathcal{W}_\mu \Phi_a. \tag{16}$$

The standard CP-conserving 2HDM potential $V_{\text{tot}}(\Phi_1, \Phi_2, T)$ consists of tree level potential $V_{\text{tree}}(\Phi_1, \Phi_2)$:

$$\begin{aligned} V_{\text{tree}}(\Phi_1, \Phi_2) = \quad & m_{11}^2 \Phi_1^\dagger \Phi_1 + m_{22}^2 \Phi_2^\dagger \Phi_2 - \left[m_{12}^2 \Phi_1^\dagger \Phi_2 + m_{12}^* \Phi_2^\dagger \Phi_1 \right] + \frac{1}{2}\lambda_1 \left(\Phi_1^\dagger \Phi_1 \right)^2 \\ & + \frac{1}{2}\lambda_2 \left(\Phi_2^\dagger \Phi_2 \right)^2 + \lambda_3 \left(\Phi_1^\dagger \Phi_1 \right) \left(\Phi_2^\dagger \Phi_2 \right) + \lambda_4 \left(\Phi_1^\dagger \Phi_2 \right) \left(\Phi_2^\dagger \Phi_1 \right) \\ & + \left[\frac{1}{2}\lambda_5 \left(\Phi_1^\dagger \Phi_2 \right)^2 + \frac{1}{2}\lambda_5^* \left(\Phi_2^\dagger \Phi_1 \right)^2 \right] \end{aligned} \tag{17}$$

and other correction terms $V_{\text{CW}}(v_1, v_2)$ and V_T. The correction terms are defined in Refs. [50,51]:

$$V_{\text{CW}}(v_1 + v_2) = \sum_i \frac{n_i}{64\pi^2} (-1)^{2s_i} m_i^4(v_1, v_2) \left[\log \left(\frac{m_i^2(v_1, v_2)}{\mu^2} \right) - c_i \right], \tag{18}$$

$$V_T = \frac{T^4}{2\pi^2} \left(\sum_{i=\text{bosons}} n_i J_B \left[\frac{m_i^2(v_1, v_2)}{T^2} \right] + \sum_{i=\text{fermions}} n_i J_F \left[\frac{m_i^2(v_1, v_2)}{T^2} \right] \right), \tag{19}$$

where μ is the renormalisation scale which we take to be 246 GeV. For a detailed overview of 2HDM scenarios and other relevant aspects, see Ref. [21].

The potential-dependent mass of fermions and bosons $m_i(v_1 + v_2)$ and the corresponding n_i, s_i, and c_i are discussed in details in Appendix B.

J_B and J_F are approximated Landau gauge up to leading orders:

$$T^4 J_B \left[\frac{m^2}{T} \right] = -\frac{\pi^4 T^4}{45} + \frac{\pi^2}{12} T^2 m^2 - \frac{\pi}{6} T (m^2)^{3/2} - \frac{1}{32} m^4 \ln \frac{m^2}{a_b T^2} + \cdots, \tag{20}$$

$$T^4 J_F \left[\frac{m^2}{T} \right] = \frac{7\pi^4 T^4}{360} - \frac{\pi^2}{24} T^2 m^2 - \frac{1}{32} m^4 \ln \frac{m^2}{a_f T^2} + \cdots, \tag{21}$$

where $a_b = 16 a_f = 16\pi^2 \exp(3/2 - 2\gamma_E)$ with γ_E being the Euler–Mascheroni constant.

When the temperature of the universe drops down to the critical temperature T_c, a second local minimum appears with the same height of the global minimum situated at $\langle \Phi_1 \rangle = \langle \Phi_2 \rangle = 0$ [52]. The critical temperature can be obtained using the following expression:

$$V_{\text{tot}}(\Phi_1 = 0, \Phi_2 = 0, T_c) = V_{\text{tot}}(\Phi_1 = v_1, \Phi_2 = v_2, T_c). \tag{22}$$

During EWPT, if ρ and P are, respectively, the energy density and pressure of the fluid determining the course of evolution of the early universe, then one gets [9]:

$$\rho = \rho_f + \rho_{\text{gauge,kin}} + \rho_{\text{Higgs}} - g^{00} \mathcal{L}_{\text{Yuk}}, \tag{23}$$

$$P = P_f + P_{\text{gauge,kin}} + P_{\text{Higgs}} - \frac{1}{3} g^{ii} \mathcal{L}_{\text{Yuk}}. \tag{24}$$

where ρ and P are the energy and the pressure density of the plasma and the the first three terms represents in the above equations the contribution from the fermionic, gauge kinetic and the Higgs sectors, respectively. We have assumed that dark matter and other components might have been present but they did not contribute much to the energy density of the universe during the particular epoch of EWPT which happened in radiation domination. The expressions for ρ_f, P_f and $\rho_{\text{gauge,kin}}, P_{\text{gauge,kin}}$ appear solely from fermionic and gauge sectors and their interactions (the stress–energy tensor for the above quantities is mentioned in Appendix A):

$$\begin{aligned}\rho_{\text{H+F+G}} &= \Big[\{\partial^0\Phi_a^\dagger - i(\mathcal{W}^0\Phi_a)^\dagger\}\partial^0\Phi_a + \{\partial^0\Phi_a + i\mathcal{W}^0\Phi_a\}\partial^0\Phi_a^\dagger\Big],\\ &-g^{00}\Big[(\partial^\alpha\Phi_a{}^\dagger)(\partial_\alpha\Phi_a) - i(\mathcal{W}^\alpha\Phi_a)^\dagger(\partial_\alpha\Phi_a) + i(\partial^\alpha\Phi_a{}^\dagger)\mathcal{W}_\alpha\Phi_a + (\mathcal{W}^\alpha\Phi_a)^\dagger\mathcal{W}_\alpha\Phi_a\Big]\\ &-g^{00}[V_{\text{tot}}(\Phi_1,\Phi_2,T)],\end{aligned} \tag{25}$$

$$\begin{aligned}P_{\text{H+F+G}} &= \Big[\{\partial^q\Phi_a^\dagger - i(\mathcal{W}^q\Phi_a)^\dagger\}\partial^q\Phi_a + \{\partial^q\Phi_a + i\mathcal{W}^q\Phi_a\}\partial^q\Phi_a^\dagger\Big]\\ &-g^{qq}\Big[(\partial^\alpha\Phi_a{}^\dagger)(\partial_\alpha\Phi_a) - i(\mathcal{W}^\alpha\Phi_a)^\dagger(\partial_\alpha\Phi_a) + i(\partial^\alpha\Phi_a{}^\dagger)\mathcal{W}_\alpha\Phi_a + (\mathcal{W}^\alpha\Phi_a)^\dagger\mathcal{W}_\alpha\Phi_a\Big]\\ &-g^{qq}[V_{\text{tot}}(\Phi_1,\Phi_2,T)].\end{aligned} \tag{26}$$

The subscript H+F+G stands for the total contribution that comes from the Higgs sector, the fermionic sector and the gauge sector. The index 00 means the first element of the metric tensor the repeated indices qq means the diagonal elements.

The early universe was flat, hence the metric $g_{\mu\nu} = (+,-,-,-)$. Furthermore, hence $\rho_{\text{H+F+G}} + P_{\text{H+F+G}}$ become:

$$\begin{aligned}\rho_{\text{H+F+G}} + P_{\text{H+F+G}} &= \partial^0\Phi_a\partial^0\Phi_a^\dagger + 2\Big[(\mathcal{W}^\alpha\Phi_a)^\dagger\mathcal{W}_\alpha\Phi_a\Big],\\ &+\Big[(\partial^0\Phi_a{}^\dagger)(\partial_0\Phi_a) - i(\mathcal{W}^0\Phi_a)^\dagger(\partial_0\Phi_a) + i(\partial^0\Phi_a{}^\dagger)\mathcal{W}_0\Phi_a\Big]\end{aligned} \tag{27}$$

where the explicit expression for $\rho_{\text{H+F+G}}$ is given as

$$\begin{aligned}\rho_{\text{H+F+G}} &= \partial^0\Phi_a\partial^0\Phi_a^\dagger + \Big[(\mathcal{W}^\alpha\Phi_a)^\dagger\mathcal{W}_\alpha\Phi_a\Big]\\ &-[V_{\text{tot}}(\Phi_1,\Phi_2,T) + \mathcal{L}_{\text{Yuk}}].\end{aligned} \tag{28}$$

The oscillations of the Higgs fields around minimum after it appeared in the course of the phase transition, are damped due to particle production by the oscillating field. The characteristic time is equal to the decay width of the Higgses and it is large in comparison with the expansion rate and the universe cooling rate. So we may assume that Higgses essentially live in the minimum, of the potential. In principle, it can be calculated numerically by the solution of the corresponding Klein–Gordon equation with damping induced by the particle production [12].

With the above assumption,

$$\rho = \dot{\Phi}_{a,\text{min}}^2 + V_{\text{tot}}(\Phi_1,\Phi_2,T) + \frac{g_*\pi^2}{30}T^4. \tag{29}$$

where g_* is the effective degrees of freedom.

The last term in Equation (29) arises from the Yukawa interaction between fermions and Higgs bosons and from the energy density of the fermions, the gauge bosons and the interaction between the Higgs and gauge bosons. This is the energy density of the relativistic particles which have not gained mass till the moment of EWPT. g_* is the effective degrees of freedom. We have assumed that the energy density consists of the two parts: the energy density of the fields $\phi(t)$s sitting at the minima of the potential and the contribution from relativistic matter.

Since for relativistic species $P = (1/3)\rho$, we can write

$$P = \frac{\dot{\Phi}_{a,\text{min}}^2}{2} + \frac{1}{3}\frac{g_*\pi^2}{30}T^4. \tag{30}$$

The oscillations of scalar fields around their minima are quickly damped, so we take the time derivative of the fields equivalent to the their derivative around the minima and

neglect higher order terms of their time derivative $\dot{\phi}^2$ and so on. Furthermore, as a result the evolution of the minima induced by the expansion of the universe is very slow.

The entropy conservation law holds when the plasma (assumed to be an ideal fluid) was in thermal equilibrium with negligible chemical potential. However, as the temperature went below T_c, EWPT happened and the universe went into a thermally nonequilibrium state. It is to be noted that one of the main consequences of EWPT is electroweak baryogenesis and, following Sakharov's principle [53], the out-of-equilibrium process is a necessary condition for successful baryogenesis.

As a result of this deviation from thermal equilibrium, the entropy conservation law is no longer valid during EWPT and, hence, a rise in the entropy production can be noticed significantly during this process.

To calculate this production, it is necessary to solve the evolution equation for energy density conservation,

$$\dot{\rho} = -3\mathcal{H}(\rho + P). \tag{31}$$

From henceforward computational analysis was used for further calculations which are discussed in the next section.

4. Entropy Release in 2HDM Scenarios

In the early universe when the temperature of universe $T \gg T_c$, the universe was in thermal equilibrium and also was dominated by relativistic species. Almost all of the fermions and bosons were massless and the contribution from those who were already massive (e.g., DM) to the total energy density of the universe was insignificant. During that epoch, the chemical potential of the massless bosons was zero, and with the assumption that chemical potential of the fermions was negligible, the entropy density per comoving volume was conserved and given by

$$s \equiv \frac{\rho_r + P_r}{T} a^3 = \text{const.}, \tag{32}$$

where the subscript r is used to indicate relativistic components. For our scenario, generalising Equation (29),

$$\rho_r + P_r \sim g_* T^4, \tag{33}$$

$g_\star$ is not constant over time; it depends on the components of the hot primordial hot soup. These two equations, Equation (32) and Equation (33), imply

$$T \sim a^{-1}. \tag{34}$$

As long as the thermal equilibrium was maintained, s remained constant. If the thermal equilibrium was not maintained at some epoch at later time, the value of s and thus $g_\star(T)a^3T^3$, might have increased as entropy can only either increase or remain constant. The contribution to entropy is dominated by a single particle species, namely by that with the largest mass in the temperature range $m(T) < T$. So for these temperatures $g_*(T)T = const.$ and the relative entropy rise is given just by a^3T^3. Since the final temperature $T_f = m(T_f)$, below which new particle species start to dominate, does not depend upon g_*, the relatives entropy rise is determined by T^3a^3. In other words, we calculate below the entropy rise over background of the constant $g_*a^3T^2$.

As the universe dropped down to T_c the Higgs potential gets degenerate minima. If the temperature drops to the mass of any component of the relativistic plasma, that component gained mass and became non-relativistic and decoupled from relativistic fluid. We are assuming this process was instantaneous and the universe was not in thermal equilibrium.There is change in $g_\star$ of the relativistic plasma. This led to increase of s.

Suppose at T_c, the scale factor was a_c and $g_\star \equiv g_{\star,\text{tot}} = 110.75$ for our 2HDM model and thus at that moment $s_c \sim g_{\star,\text{tot}}\, a_c^3\, T_c^3$. As the temperature drops down to $T \sim T_x$, the component 'x' would decoupled and thus $g_\star$ would decrease. If $g_{\star,+}$ and $g_{\star,-}$ be the $g_\star$-factor before and after the decoupling of the 'x', then change in s relative to the time of critical temperature is:

$$\frac{\delta s}{s_c} = \frac{(g_{\star,+}\, a_x\, T_x)^3 - (g_{\star,\text{tot}}\, a_c\, T_c)^3}{(g_{\star,\text{tot}}\, a_c\, T_c)^3}. \tag{35}$$

In what follows, the BSMPT C++ package, which deals with various properties and features related to 2HDM and baryon asymmetry is applied. The package was used to calculate the critical temperature for T_c and the vacuum expectation value VEV and $V_{\text{eff}}(T)$ for each benchmark points. The calculation was repeated for 4 parameter space, the first one being the benchmark points provided in the BSMPT manual. The parameters are chosen in such a way that they satisfy the limiting conditions for type-I real 2HDM. It should also be noted that we have assumed that $\text{VEV}/T_c > 1$. If this limiting assumption is varied, more benchmark points would arise, which is beyond the scope of this paper.

The differential equation Equation (31) was solved numerically by interpolating the data for $V_{\text{eff}}(T)$ for all the benchmark points and the entropy release was calculated for the same. For four different benchmark points, as mentioned in Table 1, the entropy release has been calculated with the assumption of $a_c T_c \sim 1$ and and the results are presented in Figure 1.

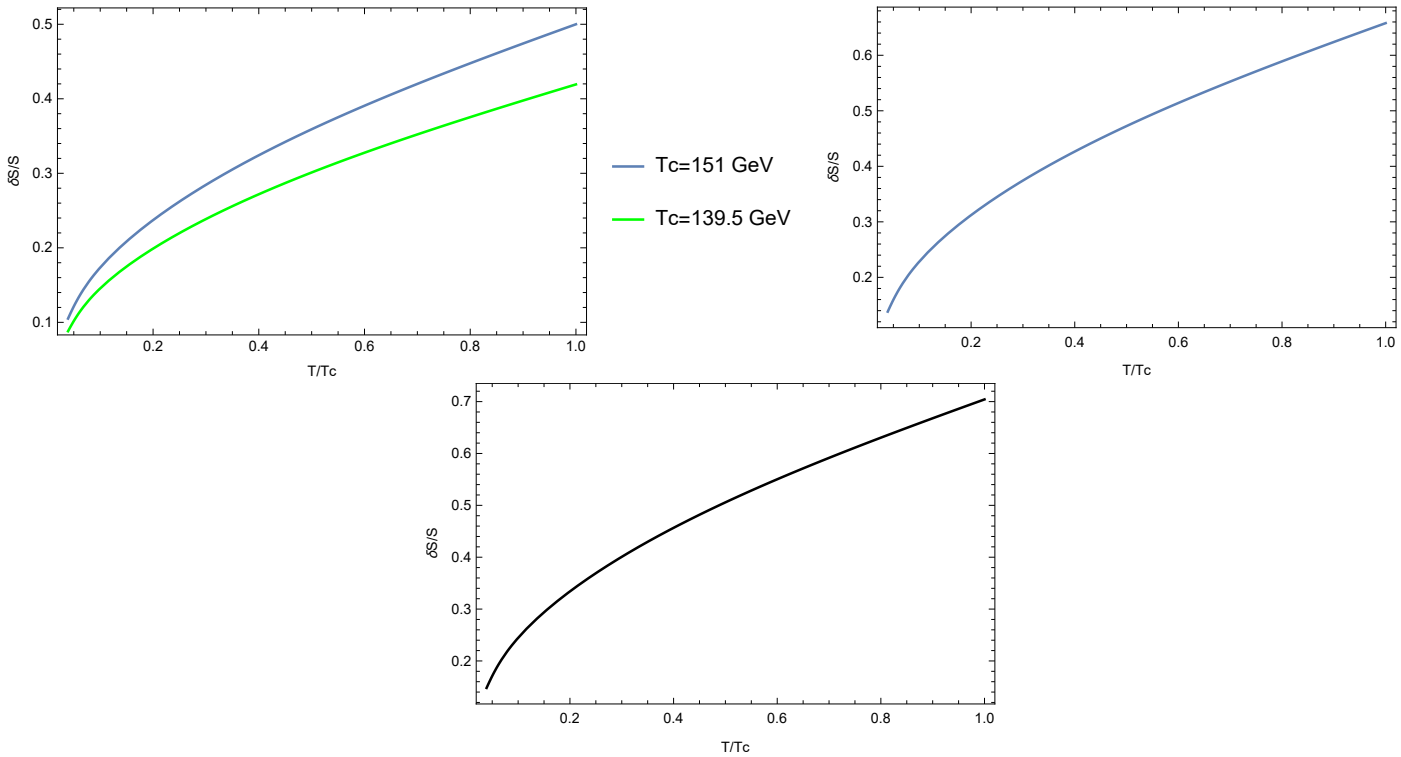

Figure 1. The entropy release for four different scenarios are shown above. The left panel shows the entropy production for $T_c = 139.5$ GeV and 151 GeV (Benchmark-IV and III, respectively). The right panel shows the entropy production for $T_c = 173.5$ GeV (blue line, Benchmark-II) and the bottom panel shows the entropy production for $T_c = 255.5$ GeV (black line, Benchmark-I).

As it is seen from Figure 1, the amount of entropy released increases as the critical temperature for EWPT increases. For example, the entropy production for $T_c = 139.5$ GeV is $\sim 41\%$, for $T_c = 151$ GeV is $\sim$52 %, for $T_c = 173.5$ GeV is $\sim$63 % and for $T_c = 255.5$ GeV is $\sim$73 %. All these results are way higher than the entropy release by EWPT in the SM which is $\sim$13% [4].

Table 1. 2HDM benchmark points for entropy production.

	m_h [GeV]		m_H [GeV]	$m_{H^\pm} = m_A$ [GeV]		$\tan\beta$
Benchmark-I	125		500	500		10
Benchmark-II	125		400	500		10
Benchmark-III	125		90	400		10
Benchmark-IV	125.09		228.17	233		6.94
	λ_1	λ_2	λ_3	λ_4	λ_5	T_c [GeV]
Benchmark-I	4.13	0.29	4.15	0	0	255.5
Benchmark-II	0.25	0.25	12.65	−1.48	−1.48	173.5
Benchmark-III	0.133	0.259	5.02	−2.51	−2.51	151
Benchmark-IV	1.22	0.29	−0.51	4.07	−3.86	139.5

The main reason for this excess in the production of entropy is the extra scalar bosons produced in the 2HDM which contributes the most to the process. It is to be noted that the contributions from lighter particles like electrons and neutrinos are similar to that of the SM.

5. Conclusions

In this paper, it is shown that the total release of entropy due to electroweak phase transition (EWPT) is very large even in the framework of minimal extension of the Standard Model (SM) of particle physics namely type-I two-Higgs-doublet model (2HDM) compared to the SM. It is a proven fact that unlike the SM where electroweak phase transition EWPT is of second order, in the mere extension of the SM, EWPT becomes a first order phase transition. An interesting fact is that as g_*, which is the effective degrees of freedom, decreases as the temperature falls down. However, as we go to a very low temperature scale, the minimum temperature takes the value of the particle mass and their contribution remains the same as that of SM.

There are two points which should be noted. First, the benchmark points are unique and they were calculated using the BSMPT package. The limiting condition of the BSMPT was set so that the vacuum expectation value (VEV) exceeds the critical temperature, T_c: $\mathrm{VEV}/T_c > 1$. All the benchmark points used here satisfy this condition. Second, in this paper, we have considered only the real sector of 2HDM. If other extensions of 2HDM such as the complex 2HDM is considered, there might be considerable change in the entropy production.

In addition, one needs to mention two effects even though they are beyond the scope of this paper. First, the entropy release due to the EWPT can considerably reduce the abundance of dark matter present in the universe before EWPT. Detailed calculation of this dilution factor for SM scenario is done in Ref. [4]. Second, bubble walls that were formed might collide and may produce primordial black holes and might lead to a sufficient entropy production. The bubble collisions are also the source of primordial gravitational wave background. These will be studied in the subsequent papers.

Author Contributions: Article by A.C. and M.Y.K. The authors contributed equally to this work. All authors have read and agreed to the published version of the manuscript.

Funding: The work of AC is funded by RSF Grant 19-42-02004. The work by M.K. has been performed with a support of the Ministry of Science and Higher Education of the Russian Federation, Project "Fundamental problems of cosmic rays and dark matter", No 0723-2020-0040.

Institutional Review Board Statement: Not applicable.

Informed Consent Statement: Not applicable.

Data Availability Statement: Not applicable.

Acknowledgments: The authors would like to thank Alexander Dolgov for carefully reading the manuscript and for several helpful discussions and comments. We acknowledge private communication with Phillipp Basler regarding BSMPT. We also thank Indrani Chakraborty, Anirban Kundu, Madhumita Santra and Soubhik Mondal for discussions.

Conflicts of Interest: There has been no conflict of interest among the authors or with any published literature.

Appendix A. Energy Momentum Tensor

$$T_f^{\mu\nu} = \sum_j i\left(\bar{\Psi}_L^{(j)}\gamma^\mu\partial^\nu\bar{\Psi}_L^{(j)} + \bar{\Psi}_R^{(j)}\gamma^\mu\partial^\nu\bar{\Psi}_R^{(j)}\right) - g^{\mu\nu}\mathcal{L}_f, \tag{A1}$$

$$\begin{aligned} T_{\text{gauge,kin}}^{\mu\nu} &= +\left[F^{B\,\mu\alpha}\partial^\nu B_\alpha - \frac{1}{4}g^{\mu\nu}F^B_{\alpha\beta}F^{B\,\alpha\beta}\right] \\ &\quad +\left[G^{i\,\mu\alpha}\partial^\nu W_\alpha - \frac{1}{4}g^{\mu\nu}G^i_{\alpha\beta}G^{i\,\alpha\beta}\right] - g\epsilon^{ijk}\left(W^{\mu j}W^k_\alpha\partial^\nu W^\alpha - W^j_\alpha W^{\nu k}\partial^\mu W^\alpha\right). \end{aligned} \tag{A2}$$

These are the stress-energy tensors for the fermioinc and the gauge sectors, respectively.

Appendix B. Masses of New Scalars

$$c_i = \begin{cases} \frac{5}{6}, & (i = W^\pm, Z, \gamma), \\ \frac{3}{2}, & \text{otherwise.} \end{cases} \tag{A3}$$

$$m_W^2 = \frac{g^2}{4}v^2, \tag{A4}$$

$$m_Z^2 = \frac{g^2 + g'^2}{4}v^2, \tag{A5}$$

$$m_\gamma^2 = 0, \tag{A6}$$

$$\bar{m}_{H^\pm}^2 = \frac{1}{2}\left(\mathcal{M}_{11}^C + \mathcal{M}_{22}^C\right) + \frac{1}{2}\sqrt{4\left(\left(\mathcal{M}_{12}^C\right)^2 + \left(\mathcal{M}_{13}^C\right)^2\right) + \left(\mathcal{M}_{11}^C - \mathcal{M}_{22}^C\right)^2}, \tag{A7}$$

$$\bar{m}_{G^\pm}^2 = \frac{1}{2}\left(\mathcal{M}_{11}^C + \mathcal{M}_{22}^C +\right) - \frac{1}{2}\sqrt{4\left(\left(\mathcal{M}_{12}^C\right)^2 + \left(\mathcal{M}_{13}^C\right)^2\right) + \left(\mathcal{M}_{11}^C - \mathcal{M}_{22}^C\right)^2}, \tag{A8}$$

where

$$c_1 = \frac{1}{48}\left(12\lambda_1 + 8\lambda_3 + 4\lambda_4 + 3\left(3g^2 + g'^2\right)\right), \tag{A9}$$

$$\begin{aligned} c_2 &= \frac{1}{48}\left(12\lambda_2 + 8\lambda_3 + 4\lambda_4 + 3\left(3g^2 + g'^2\right) + \frac{24}{v_2^2}m_t^2(T=0)\right) \\ &\quad + \frac{1}{2v_2^2}m_b^2(T=0), \end{aligned} \tag{A10}$$

where $m_t(T=0) = 172.5$ GeV and $m_b(T=0) = 4.92$ GeV. For our case $(v_3 = 0)$,

$$\mathcal{M}^C_{11} = m^2_{11} + \lambda_1 \frac{v_1^2}{2} + \lambda_3 \frac{v_2^2}{2}, \tag{A11}$$

$$\mathcal{M}^C_{22} = m^2_{22} + \lambda_2 \frac{v_2^2}{2} + \lambda_3 \frac{v_1^2}{2}, \tag{A12}$$

$$\mathcal{M}^C_{12} = \frac{v_1 v_2}{2}(\lambda_4 + \lambda_5) - m^2_{12}, \tag{A13}$$

$$\mathcal{M}^C_{13} = 0. \tag{A14}$$

Masses of h, H and A are the eigen values of the matrix

$$\bar{\mathcal{M}}^N = \left(\mathcal{M}^N\right). \tag{A15}$$

For our case $(v_3 = 0)$,

$$\mathcal{M}^N_{11} = m^2_{11} + \frac{3\lambda_1}{2} v_1^2 + \frac{\lambda_3 + \lambda_4}{2} v_2^2 + \frac{1}{2}\lambda_5 v_2^2, \tag{A16}$$

$$\mathcal{M}^N_{22} = m^2_{11} + \frac{\lambda_1}{2} v_1^2 + \frac{\lambda_3 + \lambda_4}{2} v_2^2 - \frac{1}{2}\lambda_5 v_2^2, \tag{A17}$$

$$\mathcal{M}^N_{33} = m^2_{22} + \frac{3\lambda_2}{2} v_2^2 + \frac{1}{2}(\lambda_3 + \lambda_4 + \lambda_5) v_1^2, \tag{A18}$$

$$\mathcal{M}^N_{44} = m^2_{22} + \frac{\lambda_2}{2} v_2^2 + \frac{1}{2}(\lambda_3 + \lambda_4 - \lambda_5) v_1^2, \tag{A19}$$

$$\mathcal{M}^N_{12} = 0, \tag{A20}$$

$$\mathcal{M}^N_{13} = -m^2_{12} + (\lambda_3 + \lambda_4 + \lambda_5) v_1 v_2, \tag{A21}$$

$$\mathcal{M}^N_{14} = 0, \tag{A22}$$

$$\mathcal{M}^N_{23} = 0, \tag{A23}$$

$$\mathcal{M}^N_{24} = -m^2_{12} + \lambda_5 v_1 v_2, \tag{A24}$$

$$\mathcal{M}^N_{34} = 0. \tag{A25}$$

Table A1. Field-dependent mass of all fermions.

Fermions	n_i	s_i	$m_f(T=0)$	
e	4	$\frac{1}{2}$	$\frac{y_e}{\sqrt{2}} v_k$	lepton
μ	4	$\frac{1}{2}$	$\frac{y_\mu}{\sqrt{2}} v_k$	lepton
τ	4	$\frac{1}{2}$	$\frac{y_\tau}{\sqrt{2}} v_k$	lepton
u	12	$\frac{1}{2}$	$\frac{y_u}{\sqrt{2}} v_k$	quark
c	12	$\frac{1}{2}$	$\frac{y_c}{\sqrt{2}} v_k$	quark
t	12	$\frac{1}{2}$	$\frac{y_t}{\sqrt{2}} v_k$	quark
d	12	$\frac{1}{2}$	$\frac{y_d}{\sqrt{2}} v_k$	quark
s	12	$\frac{1}{2}$	$\frac{y_s}{\sqrt{2}} v_k$	quark
b	12	$\frac{1}{2}$	$\frac{y_b}{\sqrt{2}} v_k$	quark

Table A1. *Cont.*

Bosons	n_i	s_i	$m(v)^2$	
h	1	1	eigenvalues of (A15)	Higgs
H	1	1	eigenvalues of (A15)	Higgs
A	1	1	eigenvalues of (A15)	Higgs
G^0	1	1	eigenvalues of (A15)	Goldstone
$H^\pm$	2	1	Equation (A7)	charged Higgs
$G^\pm$	2	1	Equation (A8)	charged Goldstone
Z_L	1	1	Equation (A5)	Higgs
Z_T	2	2	Equation (A5)	Higgs
W_L	2	1	Equation (A4)	Higgs
W_T	4	2	Equation (A4)	Higgs
γ_L	1	2	Equation (A6)	
γ_T	2	2	Equation (A6)	

References

1. Gorbunov, D.S.; Rubakov, V.A. *Introduction to the Theory of the Early Universe: Cosmological Perturbations and Inflationary Theory*; World Scientific Publisher: Singapore, 2011.
2. Bambi, C.; Dolgov, A.D. *Introduction to Particle Cosmology*; Springer: Berlin/Heidelberg, Germany, 2016.
3. Dolgov, A.D.; Naselsky, P.D.; Novikov, I.D. Gravitational waves, baryogenesis, and dark matter from primordial black holes. *arXiv* **2000**, arXiv:astro-ph/0009407.
4. Chaudhuri, A.; Dolgov, A. PBH evaporation, baryon asymmetry, and dark matter. *arXiv* **2020**, arXiv:2001.11219.
5. Khlopov, M. What comes after the Standard model? *Prog. Part. Nucl. Phys.* **2021**, *116*, 103824. [CrossRef]
6. Boeckel, T.; Schettler, S.; Schaffner-Bielich, J. The Cosmological QCD phase transition revisited. *Prog. Part. Nucl. Phys.* **2011**, *66*, 266–270. [CrossRef]
7. Konoplich, R.V.; Rubin, S.G.; Khlopov, M.Y. Formation of black holes in first-order phase transitions in the Universe. *Astron. Lett.* **1998**, *24*, 413–417.
8. Jedamzik, K.; Niemeyer, J.C. Primordial black hole formation during first-order phase transitions. *Phys. Rev. D* ***1999***, 59, *124014*.
9. Chen, C.H.; Chiang, C.W.; Nomura, T. Muon g-2 in two-Higgs-doublet model with type-II seesaw mechanism. *arXiv* **2021**, arXiv:2104.03275.
10. Han, X.F.; Li, T.; Wang, H.X.; Wang, L.; Zhang, Y. Lepton-specific inert two-Higgs-doublet model confronted with the new results for muon and electron g-2 anomaly and multi-lepton searches at the LHC. *arXiv* **2021**, arXiv:2104.03227.
11. Hernández, A.E.C. Fermion masses and mixings, dark matter, leptogenesis and g-2 muon anomaly in an extended 2HDM with inverse seesaw. *arXiv* **2021**, arXiv:2104.02730.
12. Chaudhuri, A.; Dolgov, A. Electroweak phase transition and entropy release in the early universe. *JCAP* **2018**, *1801*, 032. [CrossRef]
13. Bochkarev, A.I.; Kuzmin, S.V.; Shaposhnikov, M.E. Electroweak baryogenesis and the Higgs boson mass problem. *Phys. Lett. B* **1990**, *244*, 275–278. [CrossRef]
14. Basler, P.; Muhlleitner, M.; Müller, J. BSMPT v2. A Tool for the electroweak phase transition and the baryon asymmetry of the Universe in extended Higgs sectors. *arXiv* **2020**, arXiv:2007.01725.
15. Langacker, P. Introduction to the Standard Model and electroweak physics. In *The Dawn of the LHC Era (TASI 2008)*; Han, T., Ed.; World Scientific Publisher: Singapore, 2010; pp. 3–48.
16. Ginzburg, I.F.; Krawczyk, M. Symmetries of two Higgs doublet model and CP violation. *Phys. Rev. D* **2005**, *72*, 115013. [CrossRef]
17. El Kaffas, A.W.; Osl, P.; Ogreid, O.M. CP violation, stability and unitarity of the two Higgs doublet model. *Nonlin. Phenom. Complex Syst.* **2007**, *10*, 347.
18. Grzadkowski, B.; Haber, H.E.; Ogreid, O.M.; Osl, P. Heavy Higgs boson decays in the alignment limit of the 2HDM. *J. High Energy Phys.* **2018**, *12*, 056. [CrossRef]
19. Glashow, S.L.; Weinberg, S. Natural conservation laws for neutral currents. *Phys. Rev. D* **1977**, *15*, 1958. [CrossRef]

20. Paschos, E.A. Diagonal Neutral Currents. *Phys. Rev. D* **1977**, *15*, 1966. [CrossRef]
21. Branco, G.C.; Ferreira, P.M.; Lavoura, L.; Rebelo, M.N.; Sher, M.; Silva, J.P. Theory and phenomenology of two-Higgs-doublet models. *Phys. Rep.* **2012**, *516*. [CrossRef]
22. Gu, J. Learning from Higgs Physics at Future Higgs Factories. *J. High Energy Phys.* **2017**, *1712*, 153. [CrossRef]
23. Bernon, J. Scrutinizing the alignment limit in two-Higgs-doublet models. II. $m_h = 125$ GeV. *Phys. Rev. D* **2016**, *93*, 035027. [CrossRef]
24. Bernon, J. Scrutinizing the alignment limit in two-Higgs-doublet models: m_h = 125 GeV. *Phys. Rev. D* **2015**, *92*, 075004. [CrossRef]
25. Dorsch, G.C.; Huber, J.S.; Mimasu, K.; No, J.M. Hierarchical versus degenerate 2HDM: The LHC run 1 legacy at the onset of run 2. *Phys. Rev. D* **2016**, *93*, 115033. [CrossRef]
26. Bhupal Dev, P.S.; Pilaftsis, A. Erratum to: Maximally Symmetric Two Higgs Doublet Model with Natural Standard Model Alignment. *J. High Energy Phys.* **2015**, *1511*, 147. First published: *J. High Energy Phys.* **2014**, *1412*, 24. [CrossRef]
27. Pilaftsis, A. Symmetries for standard model alignment in multi-Higgs doublet models. *Phys. Rev. D* **2016**, **93**, 075012. [CrossRef]
28. Das, D.; Dey, U.K.; Pal, P.B. Quark mixing in an S_3 symmetric model with two Higgs doublets. *Phys. Rev. D* **2017**, *96*, 031701. [CrossRef]
29. Benakli, K.; Chen, Y.; Lafforgue-Marmet, G. R-symmetry for Higgs alignment without decoupling. *Eur. Phys. J. C* **2019**, *79*, 172. [CrossRef]
30. Pramanick, S.; Raychaudhuri, A. Three-Higgs-doublet model under A4 symmetry implies alignment. *J. High Energy Phys.* **2018**, *1801*, 11. [CrossRef]
31. Craig, N.; Galloway, J.; Thomas, S. Searching for signs of the second Higgs doublet. *arXiv* **2013**, arXiv:1305.2424.
32. Ferreira, P.M. The Wrong Sign limit in the 2HDM. *arXiv* **2014**, arXiv:1410.1926.
33. Modak, T. Constraining wrong-sign *hbb* couplings with $h \to \Upsilon\gamma$. *Phys. Rev. D* **2016**, *94*, 075017. [CrossRef]
34. Ferreira, P.M. Probing wrong-sign Yukawa couplings at the LHC and a future linear collider. *Phys. Rev. D* **2014**, *89*, 115003. [CrossRef]
35. Sirunyan, A.M. [CMS Collaboration] Search for Higgs boson pair production in the $\gamma\gamma b\bar{b}$ final state in pp collisions at $\sqrt{s} = 13$ TeV. *arXiv* **2018**, arXiv:1806.00408.
36. The ATLAS Collaboration. Search for a CP-odd Higgs Boson Decaying to Zh in pp Collisions at $\sqrt{s} = 13$ TeV with the ATLAS Detector. ATLAS-CONF-2016-015; CERN: Geneva, Swizerland, 2016. Available online: https://cds.cern.ch/record/2141003/files/ATLAS-CONF-2016-015.pdf (accessed on 27 April 2021).
37. The ATLAS Collaboration. Search for Additional Heavy Neutral Higgs and Gauge Bosons in the Ditau Final State Produced in 36.1 fb^{-1} of pp Collisions at $\sqrt{s}$ = 13 TeV with the ATLAS Detector. ATLAS-CONF-2017-050; CERN: Geneva, Swizerland, 2017. Available online: http://cds.cern.ch/record/2273866/files/ATLAS-CONF-2017-050.pdf (accessed on 27 April 2021).
38. The CMS Collaboration. Search for Additional Neutral Higgs Bosons Decaying to a Pair of Tau Leptons in pp Collisions at $\sqrt{s}$ = 7 and 8 TeV. CMS-PAS-HIG-14-029. CERN: Geneva, Swizerland, 2015. Available online: https://cds.cern.ch/record/2041463/files/HIG-14-029-pas.pdf (accessed on 27 April 2021).
39. The ATLAS Collaboration. Search for Heavy Resonances Decaying to a W or Z Boson and a Higgs Boson in Final States with Leptons and b-Jets in 36.1~fb^{-1} of pp Collision Data at $\sqrt{s} = 13$ TeV with the ATLAS Detector. ATLAS-CONF-2017-055; CERN: Geneva, Switzerland, 2017. Available online: https://cds.cern.ch/record/2273871/files/ATLAS-CONF-2017-055.pdf (accessed on 27 April 2021).
40. Dorsch, G.C.; Huber, S.J.; Mimasu, K.; No, J.M. Echoes of the electroweak phase transition: Discovering a second Higgs doublet through $A_0 \to ZH_0$. *Phys. Rev. Lett.* **2014**, *113*, 211802. [CrossRef]
41. Dorsch, G.C.; Huber, S.J.; No, J.M. A strong electroweak phase transition in the 2HDM after LHC8. *J. High Energy Phys.* **2013**, *1310*, 29. [CrossRef]
42. Gao, C.; Luty, M.A.; Mulhearn, M.; Neill, N.A.; Wang, Z. Searching for additional Higgs bosons via Higgs cascades. *Phys. Rev. D* **2018**, *97*, 075040. [CrossRef]
43. Bauer, M.; Carena, M.; Gemmler, K. Flavor from the electroweak scale. *J. High Energy Phys.* **2015**, *1511*, 016. [CrossRef]
44. Kling, F.; Pyarelal, A.; Su, S. Light charged Higgs bosons to AW/HW via top decay. *J. High Energy Phys.* **2015**, *1511*, 051. [CrossRef]
45. Coleppa, B.; Kling, F.; Su, S. Charged Higgs search via $AW^{\pm}/HW^{\pm}$ channel. *J. High Energy Phys.* **2014**, 1412, 148. [CrossRef]
46. Kling, F.; No, J.M.; Su, S. Anatomy of exotic Higgs decays in 2HDM. *J. High Energy Phys.* **2016**, *1609*, 093. [CrossRef]
47. Adhikary, A.; Banerjee, S.; Barman, R.K.; Bhattacherjee, B. Resonant heavy Higgs searches at the HL-LHC. *J. High Energy Phys.* **2019**, *9*, 068. [CrossRef]
48. Kling, F.; Li, H.; Pyarelal, A.; Song, H.; Su, S. Exotic Higgs decays in type-II 2HDMs at the LHC and future 100 TeV hadron colliders. *J. High Energy Phys.* **2019**, *6*, 31. [CrossRef]
49. Logan, H.E. TASI 2013 Lectures on Higgs physics within and beyond the Standard Model. *arXiv* **2013**, arXiv:1406.1786.
50. Blinov, N.; Profumo, S.; Stefaniak, T. The electroweak phase transition in the inert doublet model. *JCAP* **2015**, *7*, 028. [CrossRef]
51. Basler, P.; Krause, M.; Muhlleitner, M.; Wittbrodt, J.; Wlotzka, A. Strong first order electroweak phase transition in the CP-conserving 2HDM revisited. *J. High Energy Phys.* **2017**, *2*, 121. [CrossRef]

52. Katz, A.; Perelstein, M. Higgs couplings and electroweak phase transition. *J. High Energy Phys.* **2014**, *7*, 108. [CrossRef]
53. Sakharov, A.D. Violation of CP Invariance, C Asymmetry, and Baryon Asymmetry of the Universe. *J. Exp. Theor. Phys. Lett.* **1967**, *5*, 24–27.